



CDF/ANAL/EXOTIC/PUBLIC/8566
Version 1.1

Search for Technicolor Particles Produced in Association with W Bosons at CDF

The CDF Collaboration
<http://www-cdf.fnal.gov>
(Dated: November 7, 2006)

We present a search for technicolor particles decaying into $b\bar{b}$ and produced in association with W bosons in $p\bar{p}$ collisions at $\sqrt{s} = 1.96$ TeV. The search uses approximately 955 pb^{-1} of the dataset accumulated in the CDF detector at the Fermilab Tevatron. Events with an electron or muon, missing E_T and two jets, at least one of them b -tagged, are selected. In the case of exactly one vertex b -tag we apply a neural network filter to reject contamination from charm and light quark jets. The number of tagged events and the invariant mass distributions of $W + 2$ jets and dijets are consistent with the Standard Model expectations. We set a 95% confidence level upper limit on the production cross section times branching ratio as a function of the technicolor particle masses.

Preliminary results for Fall 2006 conferences

I. INTRODUCTION

The mechanism of electroweak symmetry breaking in the standard model is still unknown. Two of the most popular mechanisms to induce spontaneous symmetry breaking of the gauge theory, resulting in massive gauge bosons and fermions, are the Higgs mechanism and the dynamics of a new interaction such as technicolor [1, 2]. Both mechanisms predict the existence of new particles which could be produced at the Tevatron in association with a W boson.

Here we present a search for technirho production in $p\bar{p}$ collisions at $\sqrt{s} = 1.96$ TeV with subsequent decay to technipions (Fig 1). The signature $p\bar{p} \rightarrow \rho_T^\pm \rightarrow W^\pm \pi_T^0 \rightarrow \ell\nu b\bar{b}$ is produced with a cross section of order picobarns (Fig. 2) [3]. This search is also sensitive to $\rho_T^0 \rightarrow W^\pm \pi_T^\mp \rightarrow Wbc$, but it is not sensitive to ω_T^0 production associated with a photon.

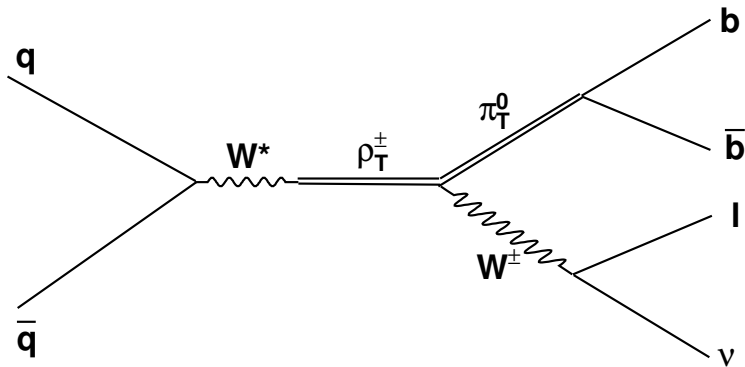


FIG. 1: Feynman diagram for $p\bar{p} \rightarrow \rho_T^\pm \rightarrow W^\pm \pi_T^0 \rightarrow \ell\nu b\bar{b}$ production.

The event signature is a final state with one high- p_T lepton, large missing transverse energy \cancel{E}_T , and two b -jets. We focus on the $W + 2$ -jet signature because the b -tagged $W + 3$ -jet signature is dominated by $t\bar{t}$ decays.

A previous search with 162 pb^{-1} of $p\bar{p}$ data at $\sqrt{s} = 1.96$ TeV from CDF resulted in an upper limit on the technirho production cross section [4]. Other searches have been published using data collected with the DØ detector [5].

II. DATA SAMPLE & EVENT SELECTION

The search uses data collected through February 2006, corresponding to 955 pb^{-1} of $p\bar{p}$ collisions at $\sqrt{s} = 1.96$ TeV.

Events selected to access the $Wb\bar{b}$ final state contain an isolated electron or muon with E_T or $p_T > 20$ GeV. Requiring $\cancel{E}_T > 25$ GeV reduces the non- W QCD contamination, which is difficult to model in events with a single b -tag. This requirement is relaxed to $\cancel{E}_T > 20$ GeV for the double b -tagged events; few non- W QCD events pass the double-tag selection. Jets are defined using a cone algorithm with radius 0.4; we count jets which have $E_T > 15$ GeV and $|\eta| < 2.0$.

A neural network b -tag filter uses jet-level variables to separate further b -jets from c -jets and light-flavor jets. The network is trained and applied to jets which have already passed the secondary vertex finding algorithm. Two neural networks are employed in series; the first uses properties of the secondary vertex itself, while the second uses jet variables independent of the tag. When the cut on the network output cuts is tuned for 90% b -jet efficiency, 65% of light-flavor jets and 50% of c -jets are rejected. The neural network b -tagger is applied only to events with exactly one secondary vertex tag. If both jets are tagged by the secondary vertex tag, the background contamination is already

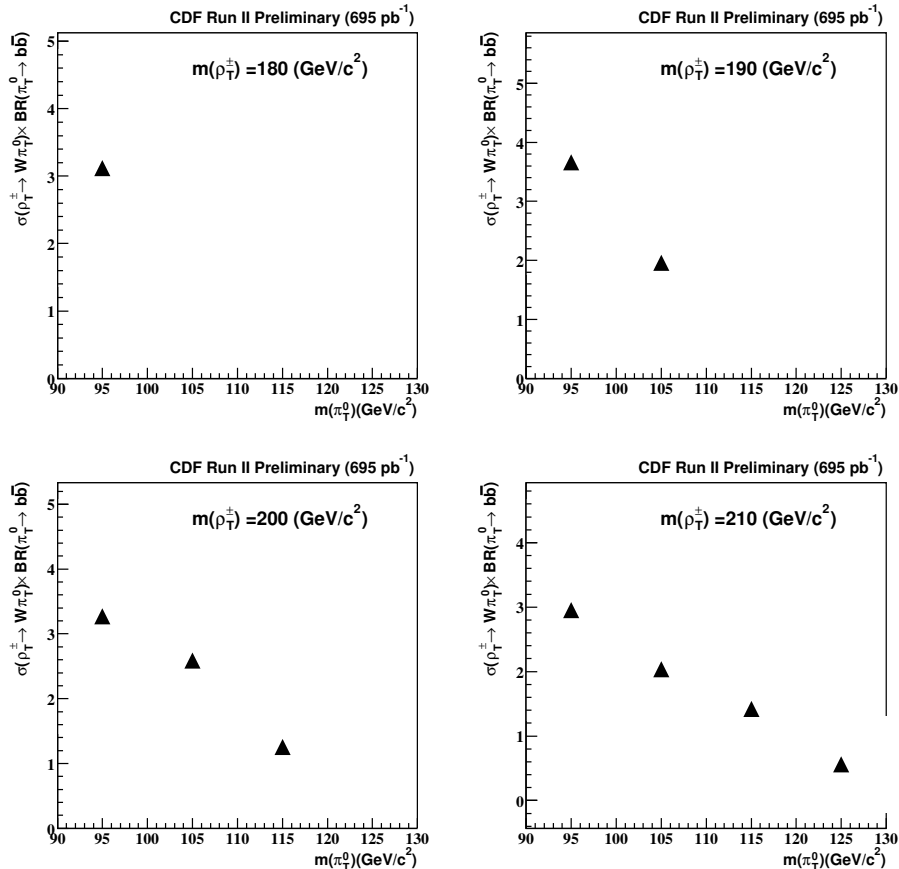


FIG. 2: Production cross section for $p\bar{p} \rightarrow \rho_T^\pm \rightarrow W^\pm \pi_T^0 \rightarrow \ell \nu b\bar{b}$ as a function of the technipion mass for various technirho masses. The calculation in PYTHIA uses the Technicolor Straw Model (TCSM).

small, and we bypass the NN filter. This also avoids the potential 10% efficiency loss per jet in the double-tag sample, which still has a limited number of events.

The dijet mass is reconstructed from the 2 jets in selected events, with both jet energies corrected for energy deposited outside the jet cones. To reconstruct the $Wb\bar{b}$ invariant mass, we need to determine the p_z of the neutrino from the W boson. After using the W mass constraint to solve for the kinematics of the $\ell\nu$ system, we take the lesser of the two p_z solutions. (If there is no real solution for p_z we take the real part of the complex solution.)

III. SIGNAL ACCEPTANCE

The signal acceptance is calculated using technicolor events generated with the PYTHIA program [6]. PYTHIA version 6.216 implements the Technicolor Straw Man Model of Lane and Mrenna [3] in leading-order calculations. We set the mass parameters of this model $M_V = M_A = 200 \text{ GeV}/c^2$. The signal acceptance is calculated in samples with $m(\rho_T)$ from 180 to 210 GeV/c^2 and with $m(\pi_T)$ from 95 to 125 GeV/c^2 . Figure 3 shows the acceptance as a function of $m(\pi_T)$ for each value of $m(\rho_T)$. The acceptance includes various calibration scale factors quantifying the difference between simulation and data, and it includes the efficiency of the high p_T -lepton triggers. No K -factor is applied to the leading-order calculation of the acceptance and cross section.

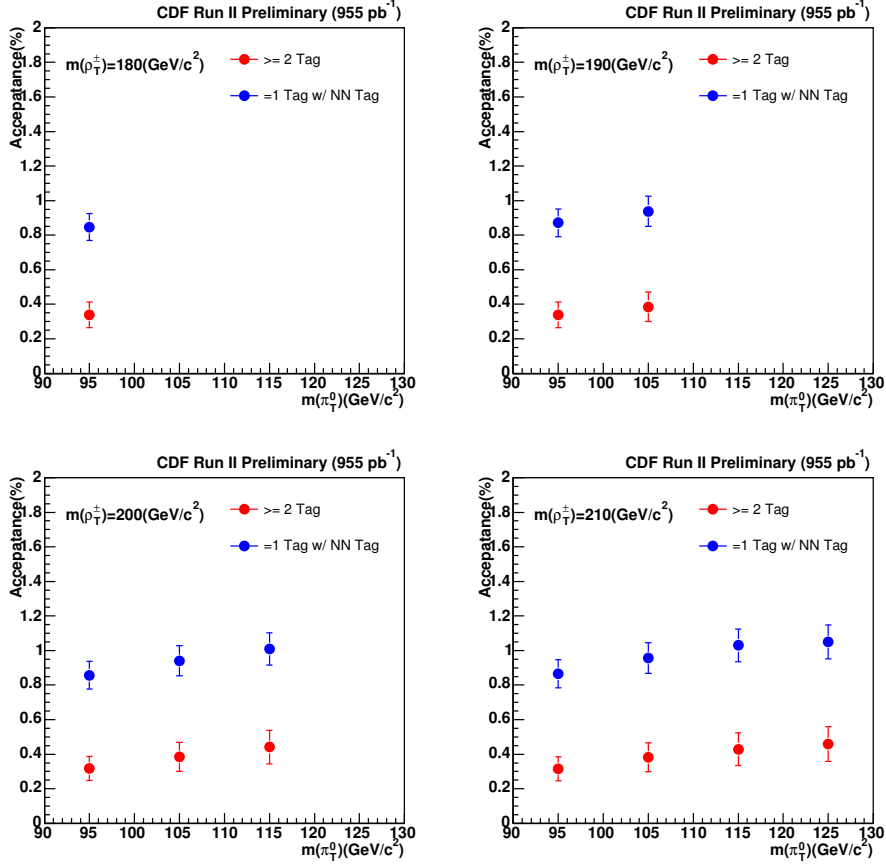


FIG. 3: Technicolor signal acceptance as a function of technipion mass $m(\pi_T)$ for each value of the technirho mass $m(\rho_T)$. The two different selections – exactly 1 NN b -tag and double vertex tag – are shown in blue and red, respectively.

Systematic uncertainties from the b -tagging efficiency, initial and final state radiation effects, and the jet energy scale are considered and summarized in Table I. Of these, the greatest effect in the selection with exactly 1 NN b -tag is the uncertain initial and final state radiation. (Because we require exactly 2 jets in the final state, a change in ISR/FSR can change the relative rate of different physics processes contributing to our selection.) The greatest systematic uncertainty in the double b -tag sample is the b -tagging efficiency as measured in the data.

	=1 tag w/ NN tag double tag	
Lepton ID	2%	2%
Trigger	< 1%	< 1%
ISR/FSR	6.7%	14%
Parton Distribution Functions	1.7%	2.6%
Jet Energy Scale	2.8%	3.9%
b -tagging	5.3%	16%

TABLE I: Summary of systematic uncertainties in the technicolor signal acceptance.

IV. BACKGROUND ESTIMATES

The composition of the b -tagged W +jets sample is dominated by the following physics processes: non-resonant W/Z +heavy flavor production, non- W QCD production, false tags of light-flavor jets in W +jets production, $t\bar{t}$ and diboson production. Determining the relative contributions and the kinematic distributions of this sample is rather tricky.

Contributions from non-resonant W/Z +heavy flavor production are estimated by calculating the heavy flavor production fraction in ALPGEN+HERWIG events with parton-jet matching [7]. The expected contribution from non- W QCD events – events with either fake isolated lepton or fake \cancel{E}_T – is estimated in \cancel{E}_T and isolation sidebands and extrapolated to the signal region. The number of false tag events can be determined by noting the signed b -tag decay length distribution of such events is roughly symmetric about 0. Then the negative tail, which is free of true heavy flavor jets, is a good estimate of the false tags with positive decay length. Other backgrounds are estimated from large samples of generated PYTHIA Monte Carlo events.

The estimated number of events in each jet multiplicity bin agrees well with the number of events observed in the data. Figure 4 shows the jet multiplicity spectra for the single NN b -tag selection and the double-tag selection.

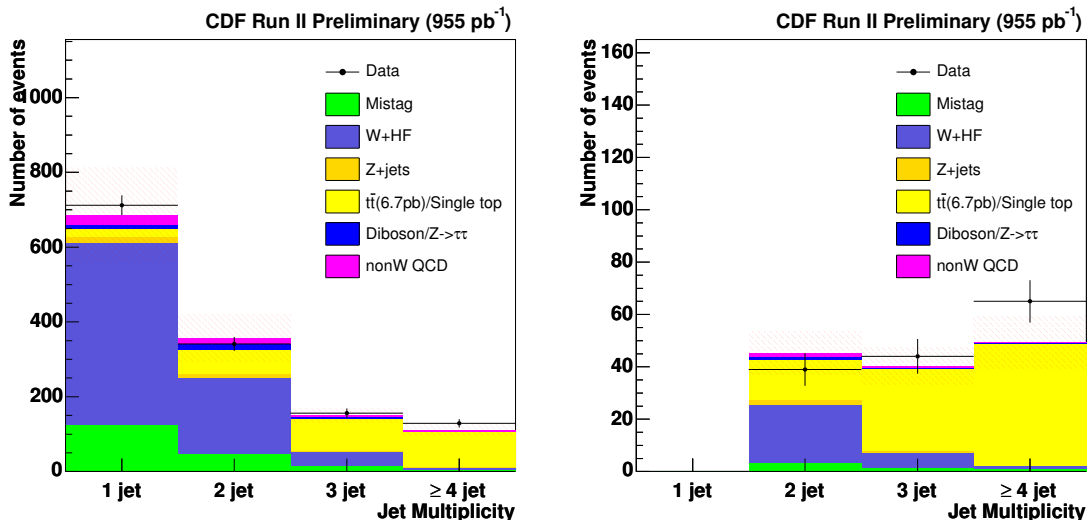


FIG. 4: Number of jets in selected events after requiring exactly 1 NN b -tag (left) or two vertex tags (right). Contributions from individual backgrounds are superimposed on the results from data.

V. RESULTS

With this event selection, we perform a direct search for a resonant mass peak in the reconstructed W + 2-jet and dijet invariant mass distributions. In fact, we consider the dijet mass distribution and a Q -value defined as $Q = m(\rho_T^\pm) - m(\pi_T^\pm) - m(W)$. The observed data spectra for these variables are consistent with the background estimate, as shown in Figs. 5 and 6.

A 2-dimensional binned maximum likelihood technique is used to derive a limit on any signal cross section times branching ratio. The background shapes are combined into two types: QCD (W +jets, non- W QCD, diboson) and top ($t\bar{t}$ and single top). We fluctuate the number of expected events separately, with Gaussian distributions for these two types having means equal to the respective background estimates and widths equal to the background uncertainties.

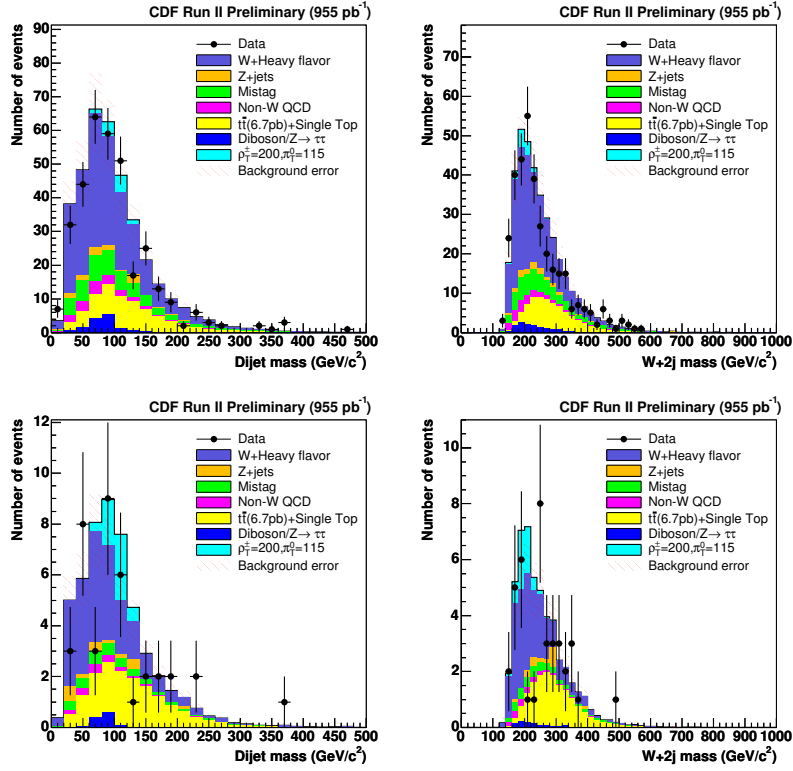


FIG. 5: Distributions of the dijet and $W + 2$ -jet invariant masses for the background estimate and observed data. Results are shown for the single NN b -tag selection (top) and double-tag selection (bottom).

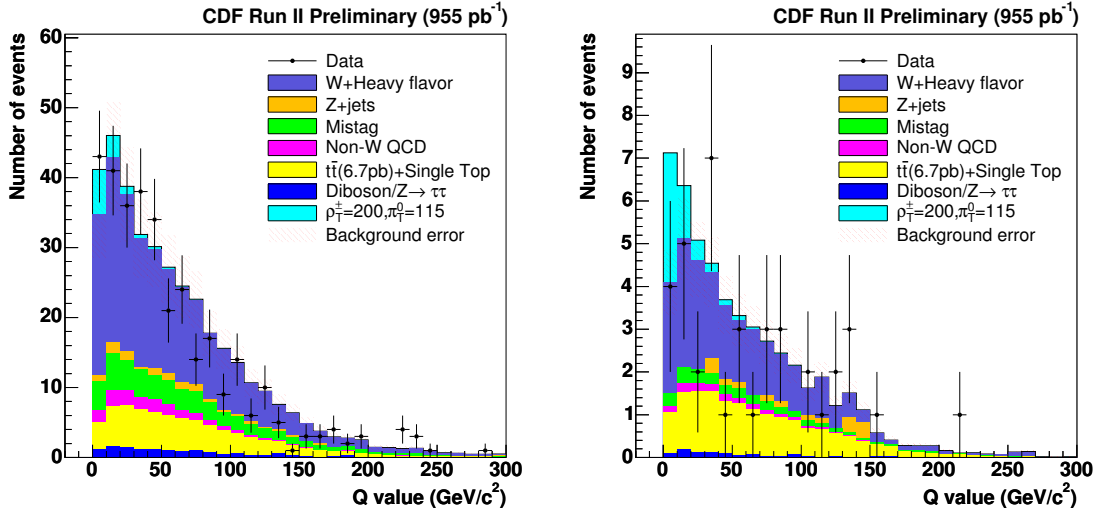


FIG. 6: Distributions of the final Q variable for the background estimate and observed data. Results are shown for the single NN b -tag selection (left) and double-tag selection (right).

A. Expected Limit from Pseudoexperiments

To estimate the sensitivity of the analysis and to optimize the selection strategy, we calculate the median expected limit in the absence of technicolor signal from a large sample of pseudo-experiments having the expected number of events.

The expected sensitivity for the two disjoint selections (exactly one NN b -tag *vs.* double-tag) is roughly equivalent, and combining the two results improves the expected limits significantly (Fig. 7).

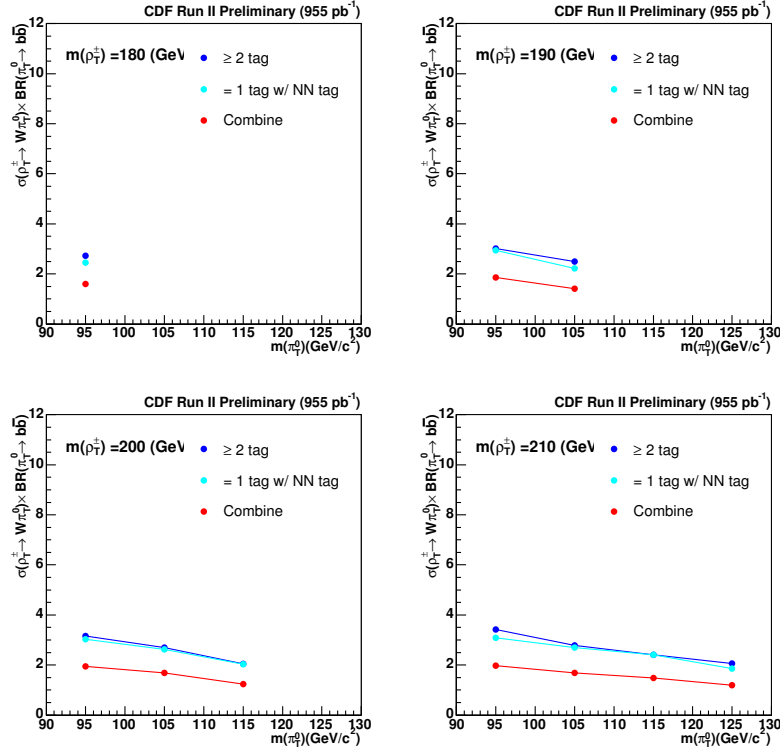


FIG. 7: Comparisons of the expected limit using the single NN b -tag selection alone (green), the double-tag selection alone (blue), and the combination (red).

In the likelihood calculation, we consider the following uncertainties to be wholly correlated between the single NN b -tag and double-tag samples: uncertainty in pre-tag signal acceptance, measurement of the b -tagging efficiency data/Monte Carlo scale factor, and uncertainty on the luminosity.

B. Observed Limit

Despite the good agreement in the predicted and observed kinematic distributions, the observed limit (Fig. 8) is somewhat larger than the expected limit from pseudoexperiments, particularly for small values of $M(\pi_T^0)$ (Fig. 9). We quantify the probability of such an outcome by defining a P -value, the fraction of background-only pseudoexperiments which yield a larger signal limit than the observed limit. We find a minimum P -value of 0.3% on the 2-D plane $m(\rho_T)$ *vs.* $m(\pi_T)$. Since we need to consider the possibility of such an effect *anywhere* in the 2-D plane, we run global pseudoexperiments to calculate the probability of so small a P -value occurring *in at least one place* in the 2-D plane. The probability of such an occurrence is 2.6%.

It would be interesting to correlate the slight excess with the Q -value used in the binned likelihood. Figure 10 shows the invariant mass distributions for various cuts on Q . It is important to understand that any apparent excess may be due to statistical fluctuations in the data or to systematic uncertainties in the background shape calculation.

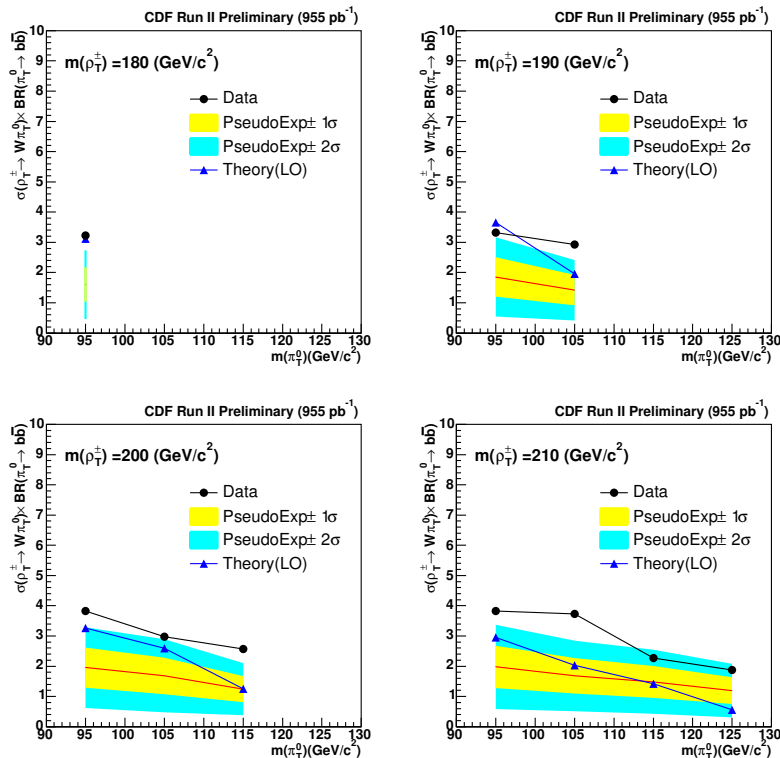


FIG. 8: Observed limit on technicolor event production as a function of the technipion mass for different values of the technirho mass. The central red line indicates the mean of the background-only pseudoexperiments, with yellow and blue bands indicating the ± 1 and $\pm 2\sigma$ bands, respectively. The theory cross section refers to the calculations from the TCSM implemented in PYTHIA. (Certain combinations of technihadron masses are kinematically inaccessible in this decay channel.)

VI. CONCLUSIONS

We have performed a search for technicolor production $p\bar{p} \rightarrow \rho_T^\pm \rightarrow W^\pm \pi_T^0 \rightarrow \ell \nu b\bar{b}$ with the CDF II detector. We find that the dataset corresponding to 955 pb^{-1} agrees with the background predictions within uncertainties. Values of the production cross section times branching fraction larger than $3 - 4 \text{ pb}$ are excluded at 95% confidence level. A small region of technicolor and technipion masses are excluded at 95% CL, based on the Technicolor Straw Man model.

VII. ACKNOWLEDGEMENTS

We thank the Fermilab staff and the technical staffs of the participating institutions for their vital contributions. This work was supported by the U.S. Department of Energy and National Science

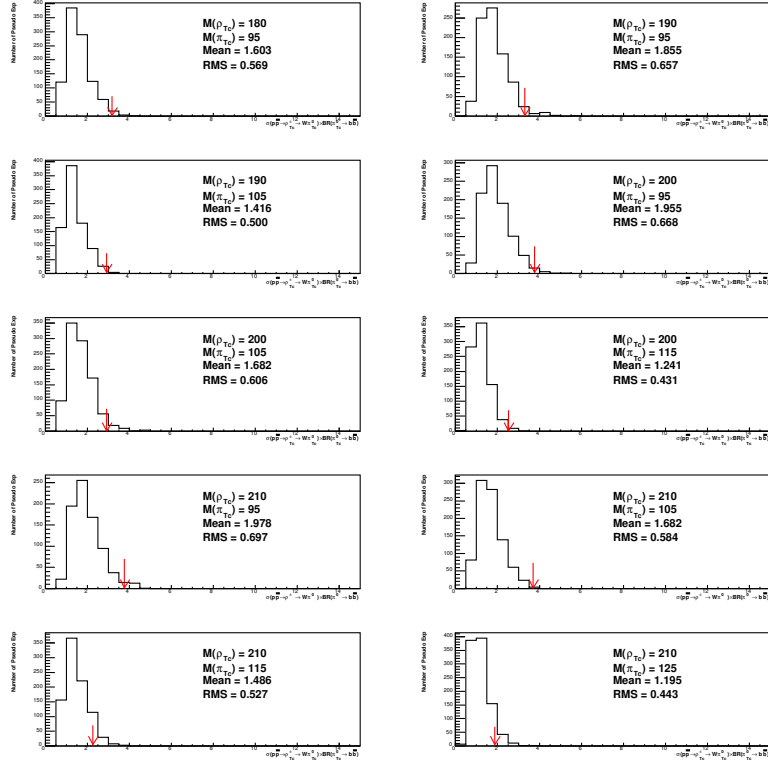


FIG. 9: Distributions of limits on signal rate in picobarns derived from background-only pseudoexperiments for various technihadron mass combinations. The median of these distributions corresponds to the expected limit; the red arrow shows the observed limit calculated for the 955 pb^{-1} dataset.

Foundation; the Italian Istituto Nazionale di Fisica Nucleare; the Ministry of Education, Culture, Sports, Science and Technology of Japan; the Natural Sciences and Engineering Research Council of Canada; the National Science Council of the Republic of China; the Swiss National Science Foundation; the A.P. Sloan Foundation; the Bundesministerium für Bildung und Forschung, Germany; the Korean Science and Engineering Foundation and the Korean Research Foundation; the Particle Physics and Astronomy Research Council and the Royal Society, UK; the Russian Foundation for Basic Research; the Comision Interministerial de Ciencia y Tecnologia, Spain; and in part by the European Community's Human Potential Programme under contract HPRN-CT-20002, Probe for New Physics.

-
- [1] S. Weinberg, “Implications of Dynamical Symmetry Breaking: An Addendum,” *Phys. Rev.* **D19** (1979) 1277-1280.
L. Susskind, “Dynamics of Spontaneous Symmetry Breaking in the Weinberg-Salam Theory,” *Phys. Rev.* **D20** strand, P. Ed n, C. Friberg, L. L (1979) 2619-2625. 2
- [2] K. D. Lane, “Technihadron production and decay in low-scale technicolor,” *Phys. Rev.* **D60** (1999) 075007, arXiv:hep-ph/9903369. 2
- [3] K. Lane and S. Mrenna, “The collider phenomenology of technihadrons in the technicolor Straw Man Model,” *Phys. Rev.* **D67** (2003) 115011, arXiv:hep-ph/0210299. 2, 3
- [4] CDF Collaboration, “Search for New Particle $X \rightarrow b\bar{b}$ at $\sqrt{s} = 1.96 \text{ TeV}$,” *CDF/PUB/EXOTIC/PUBLIC/7126* 2

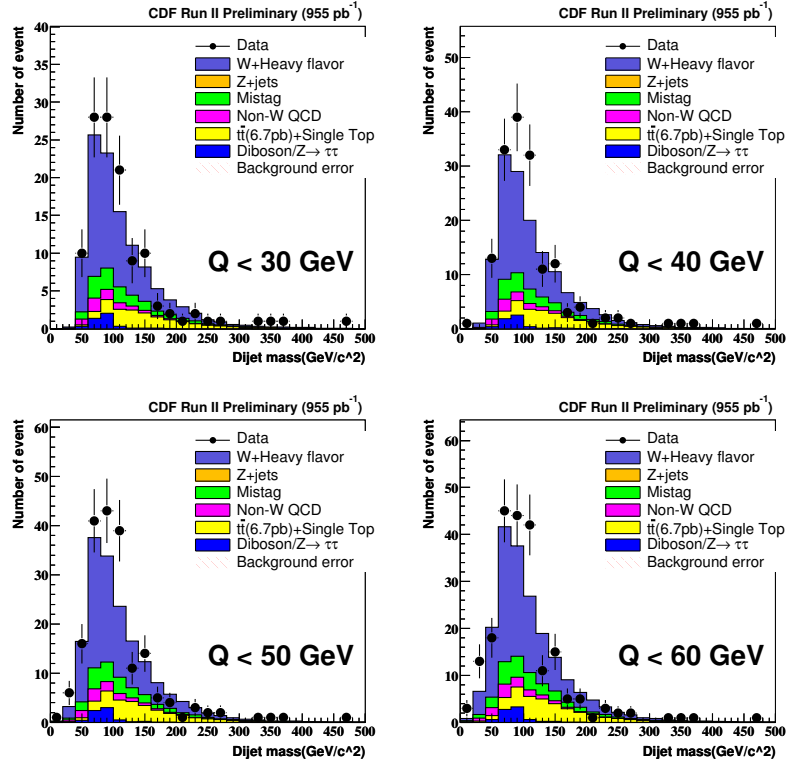


FIG. 10: Dijet invariant mass distribution in the single NN b -tag selection for various Q -value cuts. A selection with a stringent Q -value requirement seems to show a smaller excess than a selection with a loose requirement. (Note these cuts on the Q -value are for illustration purposes only; the binned likelihood is calculated for all values of Q , without a selection cut.)

- [5] DØ Collaboration, “A Search for Techniparticle Production in $p\bar{p}$ collisions at $\sqrt{s} = 1.96$ TeV in the Mode $\rho_T \rightarrow W(\rightarrow e\nu) + \omega_T$,” [DØ-CONF note 4579](#) 2
- [6] T. Sjöstrand *et al.*, “High-Energy-Physics Event Generation with PYTHIA 6.1,” [Computer Physics Commun.](#) **135** (2001) 238, [arXiv:hep-ph/0010017](#) 3
- [7] M.L. Mangano *et al.*, “ALPGEN, a generator for hard multiparton processes in hadronic collisions,” [JHEP](#) **0307:001,2003**, [arXiv:hep-ph/0206293](#). 5
- [8] G. Corcella *et al.*, “HERWIG 6.5: an event generator for Hadron Emission Reactions With Interfering Gluons,” [JHEP](#) **0101** (2001) 010, [arXiv:hep-ph/0011363](#)